Title

Inactivation of fatty acid synthase impairs hepatocarcinogenesis driven by AKT in mice and humans

Journal

Journal of Hepatology, 64(2)

ISSN

0168-8278

Authors

Li, Lei
Pilo, Giulia M
Li, Xiaolei
et al.

Publication Date

2016-02-01

DOI

10.1016/j.jhep.2015.10.004

Peer reviewed

HHS Public Access

Author manuscript

J Hepatol. Author manuscript; available in PMC 2017 February 01.

Published in final edited form as:

J Hepatol. 2016 February ; 64(2): 333–341. doi:10.1016/j.jhep.2015.10.004.

Inactivation of fatty acid synthase impairs hepatocarcinogenesis driven by AKT in mice and humans

Lei Li[1,2,†], **Giulia M. Pilo**[3,†], **Xiaolei Li**[2,4,†], **Antonio Cigliano**[5], **Gavinella Latte**[3], **Li Che**[2], **Christy Joseph**[5], **Marta Mela**[3], **Chunmei Wang**[2], **Lijie Jiang**[2], **Silvia Ribback**[5], **Maria M. Simile**[3], **Rosa M. Pascale**[3], **Frank Dombrowski**[5], **Matthias Evert**[5], **Clay F. Semenkovich**[6], **Xin Chen**[2], and **Diego F. Calvisi**[3,7]

[1]School of Pharmacy, Tongji Medical College, Huazhong University of Science and Technology, Wuhan, Hubei, China

[2]Department of Bioengineering and Therapeutic Sciences and Liver Center, University of California, San Francisco, CA, USA

[3]Department of Clinical and Experimental Medicine, University of Sassari, Sassari, Italy

[4]Department of Hepatobiliary Surgery, Xijing Hospital, The Fourth Military Medical University, Xi'an, Shaanxi, China

[5]Institut für Pathologie, Universitätsmedizin Greifswald, Greifswald, Germany

[6]Division of Endocrinology, Metabolism & Lipid Research, Washington University School of Medicine, St. Louis, MO, USA

Abstract

Background & Aims—Cumulating evidence underlines the crucial role of aberrant lipogenesis in human hepatocellular carcinoma (HCC). Here, we investigated the oncogenic potential of fatty acid synthase (FASN), the master regulator of *de novo* lipogenesis, in the mouse liver.

Methods—FASN was overexpressed in the mouse liver, either alone or in combination with activated *N-Ras*, *c-Met*, or *SCD1*, via hydrodynamic injection. Activated AKT was overexpressed via hydrodynamic injection in livers of conditional *FASN* or *Rictor* knockout mice. *FASN* was suppressed in human hepatoma cell lines via specific small interfering RNA.

[7]**Contact Information:** Diego F. Calvisi, Department of Clinical and Experimental Medicine, University of Sassari, via Padre Manzella 4, 07100 Sassari, Italy. Tel: 0039 079 228306; 0039 228305; calvisid@uniss.it.

[†]These authors contributed equally to this work

Conflict of interests: nothing to disclose

Authors' contributions

Acquisition of data; analysis and interpretation of data, drafting of the manuscript: LL, GMP, XL, AC, GL, LC, CJ, MM, CW, LJ, SR, MMS, RMP, FD, ME, XC, DFC.

Study concept and design; critical revision of the manuscript for important intellectual content; statistical analysis; obtained funding; and/or study supervision: CFS, ME, XC, and DFC.

Results—Overexpression of *FASN*, either alone or in combination with other genes associated with hepatocarcinogenesis, did not induce histological liver alterations. In contrast, genetic ablation of *FASN* resulted in the complete inhibition of hepatocarcinogenesis in *AKT*-overexpressing mice. In human HCC cell lines, FASN inactivation led to a decline in cell proliferation and a rise in apoptosis, which were paralleled by a decrease in the levels of phosphorylated/activated AKT, an event controlled by the mammalian target of rapamycin complex 2 (mTORC2). Downregulation of AKT phosphorylation/activation following FASN inactivation was associated with strong inhibition of rapamycin-insensitive companion of mTOR (Rictor), the major component of mTORC2, at post-transcriptional level. Finally, genetic ablation of Rictor impaired AKT-driven hepatocarcinogenesis in mice.

Conclusions—FASN is not oncogenic *per se* in the mouse liver, but is necessary for AKT-driven hepatocarcinogenesis. Pharmacological blockade of FASN might be highly useful in the treatment of human HCC characterized by activation of the AKT pathway.

Keywords

hepatocellular carcinoma; lipogenesis; fatty acid synthase; AKT; Rictor

Introduction

Deregulated fatty acid biosynthesis, also known as *de novo* lipogenesis, is a key aberration in cancer [1–3]. It provides rapidly proliferating cancer cells with a continuous supply of lipids and lipid precursors that are needed for membrane production, energy generation, and lipid-based post-transcriptional modifications of proteins [1–3]. At the molecular level, *de novo* lipogenesis is characterized by upregulation in tumor cells of lipogenic enzymes, including adenosine triphosphate citrate lyase (ACLY), acetyl-CoA carboxylase (ACAC), fatty acid synthase (FASN), and stearoyl-CoA desaturase 1 (SCD1) [1–3]. FASN, the enzyme responsible for production of long-chain fatty acids from acetyl-coA and malonyl-CoA, is the most investigated lipogenic protein in cancer [1–3]. FASN levels are elevated in many tumor types, where they significantly correlate with cancer biological aggressiveness and unfavorable prognosis [1–3]. In addition, upregulation of FASN occurs in preneoplastic and pre-invasive lesions of various organs [1–3]. Also, FASN blockade triggers tumor growth restraint and massive apoptosis in numerous *in vitro* and *in vivo* models [1–3]. Furthermore, FASN overexpression induces the development of prostate intraepithelial neoplasia in transgenic mice, thus acting as a *bona fide* oncogene in prostate cancer [4]. Similarly, overexpression of FASN induces a cancer-like phenotype in non-tumorous breast cell lines [5].

In hepatocellular carcinoma (HCC), aberrant expression of lipogenic enzymes including FASN has been linked both to tumor development and progression. For instance, overexpression of FASN occurs in liver preneoplastic lesions from rat models of chemically- and hormonally-induced hepatocarcinogenesis [6]. Similarly, sustained lipogenesis and FASN upregulation characterize human liver clear cell foci, whose preneoplastic nature has been hypothesized [7]. Also, levels of FASN and other lipogenic proteins as well as polymorphisms in lipogenic genes are associated with poor outcome in HCC patients [8–12]. In addition, FASN suppression has been shown to be detrimental for

HCC growth *in vitro* [10,13,14]. Despite this body of evidence, key questions about FASN in HCC remain unanswered. Virtually all functional studies on FASN in HCC have been performed in HCC cell lines so far. Thus, it is unknown whether FASN contributes to liver tumor development and/or progression *in vivo*.

Here, we determined the functional contribution of FASN to liver cancer development *in vivo* by overexpressing *FASN*, either alone or in association with oncogenes that have been associated with hepatocarcinogenesis, in the mouse liver via hydrodynamic gene delivery. Furthermore, we assessed the importance of FASN on AKT-driven hepatocarcinogenesis by overexpressing *AKT* in *FASN*-depleted mice.

Materials and methods

Constructs and reagents

pT3-EF1α, pT3-EF1α-HA-myr-AKT1, pT2-Caggs-N-RasV12, pT3-EF1a-V5-c-Met, pT3-EF1α-Cre, and pCMV/sleeping beauty transposase (SB) plasmids were described previously [10,15–18]. Human(h) *FASN* (ID: 6172538) and h*SCD1* (ID: 3844850) full length cDNAs were from Open Biosystems (Lafayette, CO), and cloned into pT3-EF1a vectors via the Gateway polymerase chain reaction (PCR) cloning strategy (Invitrogen, Carlsbad, CA). Plasmids were purified using the Endotoxin free Maxi prep kit (Sigma-Aldrich, St. Louis, MO) before injecting into mice.

Hydrodynamic injection, mouse monitoring

FASN$^{fl/fl}$ mice (in C57BL/6 background) were previously described [19]. *AlbCre* mice [20], purchased from Jackson Laboratory (Bar Harbor, ME), were crossed with *FASN*$^{fl/fl}$ mice to generate liver-specific FASN null mice (*AlbCre;FASN*$^{fl/fl}$ mice). Hydrodynamic injections were performed as reported previously [21]. To determine the oncogenic potential of lipogenic enzymes, 20 μg of the plasmids encoding the gene(s) of interest along with sleeping beauty transposase in a ratio of 25:1 were diluted in 2 ml saline (0.9% NaCl) for each mouse. Saline solution was filtered through a 0.22 μm filter and injected into the lateral tail vein of six- to eight-week-old mice in 5–7 seconds. To study the requirement of FASN for AKT-driven hepatocarcinogenesis, two approaches were employed. In the first approach, six- to eight-week-old *FASN*$^{fl/fl}$ mice were injected with AKT (8μg) and Cre recombinase (40μg). Additional *FASN*$^{fl/fl}$ mice were injected with AKT (8μg) and pT3 (40μg) as control. In the second approach, AKT (20μg) was injected into four months old *AlbCre;FASN*$^{fl/fl}$ mice and control *FASN*$^{fl/fl}$ mice. Rictor$^{fl/fl}$ mice [22] were purchased from Jackson Laboratory. To determine the importance of Rictor on AKT-driven hepatocarcinogenesis, AKT (8μg) together with Cre (40μg) was injected into 6 to 8 weeks old Rictor$^{fl/fl}$ mice. AKT (8μg) together with pT3EF1a (40μg) was injected into Rictor$^{fl/fl}$ mice as control. Mice were housed, fed, and monitored in accordance with protocols approved by the Committee for Animal Research at the University of California, San Francisco.

Detailed description of Materials and methods is provided as Supplementary material.

Results

FASN is not oncogenic per se in the mouse liver

To determine whether FASN has oncogenic potential *in vivo*, we hydrodynamically delivered the pT3-EF1α-hFASN plasmid to the mouse liver. Overexpression of human *FASN* alone did not trigger tumor formation or histological alterations in mice up to 40 weeks post-injection (n=6). Macroscopically and histologically, FASN-injected livers were indistinguishable from empty plasmid-injected or un-injected livers (Fig. 1A), and did not show any sign of lipogenesis when compared with control mice (Fig. 1A). Scattered hepatocytes positive for human FASN immunolabeling were detected in FASN-injected livers (Fig. 1A, inset). Overexpression of human FASN was also confirmed by real-time RT-PCR (Fig. 1A). Similarly, co-expression of *FASN* with *c-Met* (Fig. 1B; n=5) or an oncogenic form of *N-Ras* (*N-RasV12*; Fig. 1C; n=5) did not result in any liver anomaly at the same time point. Furthermore, *FASN* transfection was unable to drive tumor development or lipid accumulation in the mouse liver when co-injected with another lipogenic enzyme, *SCD1* (Fig. 1D; n=5). Overexpression of *SCD1* alone was also unsuccessful in inducing histological alterations in the mouse liver (Fig. 1E; n=5). Consequently, no significant difference in liver weight (Fig. 1F) or proliferation rate (Fig. 1G) was detected in the various mouse models when compared with wild-type mice and mice injected with empty vector. Altogether, the present findings indicate that overexpression of FASN does not promote hepatocyte malignant transformation and tumor development in the mouse liver.

FASN is required for AKT-induced liver steatosis and tumor development

To determine whether AKT-driven hepatic steatosis depends on FASN-mediated lipogenesis, we overexpressed the activated form of *AKT1* (*myr-AKT1*) while simultaneously deleting FASN in the hepatocytes. To achieve this goal, we hydrodynamically transfected *FASN*$^{fl/fl}$ mice with myr-*AKT1* and *Cre* recombinase (referred to as AKT/Cre mice; n=5). As a control, we hydrodynamically transfected FASN$^{fl/fl}$ mice with AKT and pT3 empty vector (referred to as AKT mice; n=5) (Fig. 2A). Subsequently, mice were harvested 4 weeks post hydrodynamic injection, when livers overexpressing *myr-AKT1* display extensive lipid accumulation [10]. We found that livers from AKT mice were macroscopically pale and spotty (Fig. 2B), equivalent to those described when *AKT* was overexpressed in wild-type mice [10]. Microscopically, ~60% of the liver parenchyma of AKT mice was occupied by lipid-rich hepatocytes exhibiting strong immunolabeling for the injected construct (HA-tagged myr-AKT1), FASN, and phosphorylated/activated AKT (p-AKT; Fig. 2B). In contrast, livers from AKT/Cre mice were macroscopically normal, and indistinguishable from un-injected wild-type or *FASN*$^{fl/fl}$ mouse livers (Fig. 2C). Only a few (3–5%) lipid-rich hepatocytes were positive for the injected construct (Fig. 2C). Importantly, almost all lipid-rich hepatocytes exhibiting immunolabeling for HA-tag did not display immunoreactivity for FASN, confirming the successful elimination of *FASN* by Cre recombinase in HA-tag expressing cells (Fig. 2C). The same lipid-rich hepatocytes exhibited low or absent p-AKT immunolabeling (Fig. 2C). In addition, Oil-Red-O (ORO) staining revealed extensive lipid droplet accumulation in AKT (Fig. 2B), but not AKT/Cre livers (Fig. 2C). Furthermore, only a few of the lipid-rich, HA-positive hepatocytes from AKT/Cre

mice were proliferating (Fig. 2C, inset), whereas numerous HA-transfected hepatocytes from AKT mice were in active proliferation (Fig. 2B, *inset*). Downregulation of AKT and related lipogenesis in AKT/Cre livers was also confirmed by Western blotting and/or real-time RT PCR (Supplementary Fig. 1). As an additional control group, we injected AKT and Cre recombinase into wild-type mice: a marked lipid accumulation in hepatocytes of these mice was detected (data not shown), indicating that the phenotype observed in AKT/Cre mice specifically depends on the ablation of *FASN* by Cre.

AKT overexpression leads to malignant liver tumor formation by 22–32 weeks post-injection [10]. To determine whether FASN expression is required for AKT-driven hepatocarcinogenesis, we aged AKT (n=6) and AKT/Cre (n=5) mice. Two AKT mice were sacrificed 22 weeks post-injection due to liver tumor burden, while all remaining mice being euthanized 31 weeks post-injection. All AKT mice showed an enlarged liver with a consequent increased liver weight when compared to control mice (Fig. 3A; Supplementary Fig. 2). In striking contrast, none of the AKT/Cre mice exhibited either liver enlargement or increased liver weight (Fig. 3D; Supplementary Fig. 2). Histologically, most of the liver parenchyma of AKT mice was occupied by multiple hepatocellular tumors (Fig. 3B,C). All AKT/Cre mice showed instead the absence of preneoplastic and neoplastic lesions (Fig. 3E). Single, lipid-rich cells were detected in otherwise normal appearing livers in AKT/Cre mice (Fig. 3F). At the cellular level, livers from AKT mice displayed a significantly higher proliferation rate when compared with AKT/Cre livers (Supplementary Fig. 2), whereas no differences in apoptosis were found between the two mouse models (Supplementary Fig. 2). Both proliferation and apoptosis degree detected in AKT/Cre livers were equivalent to those in control mice (Supplementary Fig. 2).

To further characterize how FASN regulates lipid metabolism in the liver, levels of triglyceride (TG) and cholesterol esters (CE) were assayed in livers from control, AKT, and AKT/Cre mice at this time point (Supplementary Fig. 3). As expected, AKT livers showed the highest levels of TG and CE. Fatty acid composition analysis showed that monounsaturated fatty acids (MUFA), including palmitoleic acid (16:1) and oleic acid (18:1), were higher in both TG and CE in AKT liver tissues, whereas saturated fatty acids (SFA) levels were lower. In contrast, AKT/Cre livers did not show increased TG and CE levels when compared with control livers. Increased MUFA and decreased SFA levels driven by AKT overexpression were significantly attenuated in AKT/Cre livers (Supplementary Fig. 3).

To complement this study, we generated liver specific *FASN* knockout mice (*AlbCre;FASN*$^{fl/fl}$ mice) by hydrodynamically injecting *myr-AKT1* into *AlbCre;FASN*$^{fl/fl}$ mice and control *FASN*$^{fl/fl}$ littermates (Supplementary Fig. 4). Similar to what we observed previously, *FASN* ablation completely inhibited AKT-driven hepatic steatosis and tumorigenesis (Supplementary Fig. 4).

Altogether, the present data indicate that FASN expression is indispensable for AKT-induced steatosis and hepatocarcinogenesis.

FASN deletion impairs AKT activation by Rictor suppression

Next, we investigated the molecular mechanisms associated with inhibition of hepatocarcinogenesis in AKT/Cre mice. For this purpose, levels of the main downstream effectors of AKT were assessed by immunohistochemistry, Western blotting, and/or real-time RT-PCR (Fig. 4, 5, Supplementary Fig. 5). Levels of FASN and AKT were significantly higher in AKT mice when compared with AKT/Cre mice. Similarly, levels of p-AKT at serine 472 (p-AKTser472; homolog to human serine 473) were significantly higher in AKT mice than AKT/Cre mice. Levels of AKT downstream effectors, including ACAC, ACLY, SCD1, nuclear/activated sterol regulatory element-binding protein 1 (SREBP1), and pyruvate kinase M2 isoform (PKM2) were highest in AKT mice, whereas lactate dehydrogenase A/C (LDHA/C) displayed equivalent protein levels in AKT and AKT/Cre livers (Fig. 4, 5, Supplementary Fig. 5). As concerns mTORC1 members, levels of phosphorylated/inactivated 4E-binding protein 1 (4E-BP1) and phosphorylated/activated AMP-activated protein kinase α (AMPKα) were highest in control livers and lowest in AKT/Cre livers, whereas levels of regulatory-associated protein of mTOR (Raptor) were equivalent in control and AKT/Cre livers and lowest in AKT mice (Fig. 4, 5, Supplementary Fig. 5). Since phosphorylation of AKT at ser472/3 depends on mammalian target of rapamycin complex 2 (mTORC2) [23], we assessed whether FASN depletion affect mTORC2 levels. For this purpose, the levels of the mTORC2 main component, rapamycin insensitive companion of mTOR (Rictor) were assessed by Western blotting. Notably, a strong induction of Rictor characterized AKT livers, whereas low/absent Rictor levels were detected in AKT/Cre livers (Fig. 5, Supplementary Fig. 5).

To substantiate the latter findings, FASN expression was modulated in human hepatoma cell lines and Rictor levels were assessed. *FASN* silencing via specific small interfering RNA (siRNA) resulted in Rictor downregulation HLF and HepG2 cells, whereas levels of Raptor and other mTORC1 members (phosphorylated/activated ribosomal protein S6, p-4EBP1), and proteins involved in lipogenesis (activated/nuclear SREBP1) and glycolysis (PKM2) were either unaffected or upregulated by FASN depletion (Fig. 6A,B, Supplementary Fig. 6, 7). Rictor downregulation occurred at post-transcriptional level, as only protein but not mRNA levels of Rictor decreased following *FASN* knockdown (Fig. 6A,B, Supplementary Fig. 6–8). *FASN* silencing also triggered downregulation of p-AKT in both cell lines, without affecting total AKT levels (Fig. 6A,B, Supplementary Fig. 6, 7). Equivalent results were obtained when HLF and HepG2 cell lines were subjected to administration of the FASN chemical inhibitor, C75 (Supplementary Fig. 9). Recently, it has been shown that ELOVL5 regulates Rictor levels in hepatoma cells [24]. To determine whether the same applies for AKT/Cre mice, ELOVL5 levels were assessed in AKT and AKT/Cre mice. ELOVL5 levels were equivalent in the two mouse models (Fig. 6, Supplementary Fig. 5). Similarly, *FASN* depletion in HLF and HepG2 cells did not trigger ELOVL5 dowregulation (Fig. 6A, Supplementary Fig. 6, 7), suggesting that FASN promotes Rictor downregulation via ELOVL5-independent mechanisms. In addition, we assessed the importance of Rictor in HLF cells depleted of FASN (Supplementary Fig. 10). FASN suppression via siRNA decreased cell proliferation and augmented apoptosis in HLF cells. However, when *FASN* suppression was coupled to concomitant overexpression of *Rictor* cDNA via transient transfection, the growth restraint induced by FASN knockdown, both in terms of

proliferation and apoptosis, was significantly decreased in HLF cells (Supplementary Fig. 10). These results indicate that FASN is necessary for AKT-driven carcinogenesis in the mouse liver, presumably via its ability to positively regulate Rictor, the AKT upstream activator.

Rictor deletion suppresses AKT activity and AKT-driven hepatocarcinogenesis in mice

The role of Rictor in AKT-driven hepatocarcinogenesis was further investigated *in vivo*. *Rictor*$^{fl/fl}$ mice were hydrodynamically injected with myr-*AKT1* and *Cre* recombinase (indicated as AKT/Cre mice; n=8) in order to overexpress *myr-AKT1* while simultaneously deleting Rictor in hepatocytes. As control, Rictor$^{fl/fl}$ mice were injected with AKT and pT3 empty vector (AKT mice; n=10). Subsequently, a group of AKT and AKT/Cre mice (n=4 each) was harvested 4 weeks post-injection. While AKT livers were occupied by clusters of lipid-rich hepatocytes showing strong immunolabeling for HA-tagged myr-AKT1 and p-AKT, only a few lipid-rich hepatocytes were detected in AKT/Cre livers (Supplementary Fig. 11). Importantly, AKT/Cre hepatocytes displayed immunoreactivity for HA-tagged myr-AKT1 but not for p-AKT (Supplementary Fig. 11), indicating that deletion of Rictor impairs AKT phosphorylation/activation in the mouse liver.

A second group of AKT (n=6) and AKT/Cre (n=4) mice in the *Rictor*$^{fl/fl}$ background was aged and sacrificed 22 weeks post-injection. All AKT mice showed the presence of multiple hepatocellular tumors throughout the liver parenchyma, whereas no preneoplastic and neoplastic lesions were detected in AKT/Cre mice (Fig. 7). Once again, AKT/Cre hepatocytes that were positive for HA-tagged-Myr-AKT1 did not display p-AKT immunolabeling (Fig. 7). Altogether, the present results indicate that Rictor is indispensable for AKT activity and AKT-dependent hepatocarcinogenesis in the mouse liver.

Overexpression of FASN, phosphorylated-AKT, and Rictor in human hepatocellular carcinoma

Finally, given the strong anti-neoplastic effect induced by *FASN* depletion in mouse livers overexpressing *AKT* and the molecular mechanisms involved, we assessed the frequency of HCC patients who might eventually benefit from FASN inhibition. Thus, levels of FASN, p-AKT, and Rictor were analyzed in a collection of human HCC specimens (n = 88; Supplementary Table 1) by immunohistochemistry (Fig. 8). Furthermore, levels of ELOVL5 were evaluated to further investigate the relationship between the latter protein and Rictor. Higher immunolabeling for FASN, p-AKT, and Rictor was found in 81.8%, 60.2%, and 21.6% of HCC specimens, respectively, when compared with surrounding non-tumorous livers. Importantly, all HCC specimens showing p-AKT and Rictor overexpression also exhibited elevated FASN levels. Also, all samples showing induction of Rictor displayed elevated p-AKT. Furthermore, 44 of 72 (61.1%; $P < 0.02$), 35 of 53 (66.03%; $P < 0.005$), and 12 of 19 (63.1%; $P < 0.05$) liver tumors displaying induction of FASN, p-AKT, and Rictor, respectively, belonged to the HCC subset with poorer outcome, linking the overexpression of these proteins to a dismal prognosis in HCC. No association between FASN, p-AKT, and Rictor staining patterns and other clinicopathological features of the patients was detected. Upregulation of ELOVL5 occurred in 28.4% of HCC; however, only 5 of 25 (20%) specimens with elevated ELOVL5 simultaneously displayed Rictor

upregulation. No association was found between ELOVL5 levels and patients' clinicopathological features. The present data indicate that induction of FASN, p-AKT, and Rictor proteins occurs frequently in human HCC, mainly in the tumor subset with the most unfavorable outcome.

Discussion

In this study, we addressed the role of FASN along hepatocarcinogenesis for the first time. We showed here that overexpression of FASN, either alone or in association with N-Ras, c-Met or SCD1, is not sufficient to malignantly transform hepatocytes and drive liver tumor development. Nevertheless, our findings imply a pivotal function of FASN in supporting hepatocarcinogenesis induced by the AKT protooncogene. This assumption is based on the complete inhibition of preneoplastic and neoplastic liver lesion development in AKT mice where FASN was genetically deleted. Whether the inhibition of FASN in AKT-overexpressing hepatocytes is detrimental for their growth due to mechanisms related to the metabolism and/or the survival signals activated by FASN remains to be determined. Noticeably, it has been previously reported that AKT-overexpressing cells are incapable of survival and proliferation *in vitro* when *de novo* fatty acid synthesis is inhibited [25]. This "metabolic addiction" to aberrant lipogenesis is fully recapitulated in our *in vivo* model.

Besides these effects on liver cancer cell metabolism, our data indicate that FASN regulates important molecular events. Indeed, we found that FASN is involved in the control of AKT activation via regulation of Rictor, the main mTORC2 component. The control of Rictor and, consequently, AKT phosphorylation/activation by FASN, was detected both in mouse livers and human hepatoma cell lines, implying that this molecular mechanism is conserved among species. Also, the regulation of p-AKT by FASN has been previously demonstrated in human osteosarcoma, colorectal, and ovarian cancer cell lines [26–28].

Although the precise molecular event triggered by FASN that is responsible for Rictor regulation remains poorly defined, our present data indicate that FASN does not affect mRNA levels of Rictor, but acts post-transcriptionally. In addition, despite a recent report showing that Rictor levels are modulated by ELOVL5 in HepG2 cells [24], our data seem to exclude that FASN acts via ELOVL5 in liver cancer cells both *in vivo* and *in vitro*. Indeed, ELOVL5 was neither downregulated following *FASN* deletion in mice nor in *FASN*-depleted hepatoma cell lines. Also, no relationship between Rictor and ELOVL5 levels was found in human HCC samples. Furthermore, ELOVL5 was found to affect the expression of Rictor at mRNA level [24], whereas *Rictor* mRNA expression remained unmodified following *FASN* suppression in hepatoma cells. Also, our preliminary findings indicate the absence of increased ubiquitination of Rictor in *FASN*-deprived hepatoma cell lines (Supplementary Fig. 12). Altogether, the present findings strongly suggest that molecular mechanism independent of ELOVL5 activity and proteolysis are responsible for Rictor downregulation in *FASN*-depleted cells. Clearly, additional studies are required to fully elucidate the molecular mechanisms downstream of FASN regulating Rictor and mTORC2 activation. As FASN is a major regulator of lipid metabolism, lipidomic approaches are necessary to identify the fatty acids and lipids that are specifically modulated by FASN in HCC cells. The functional contribution of the differentially regulated lipids to HCC cell

growth and Rictor modulation are currently under investigation. Another possible mechanism whereby fatty acids may regulate Rictor expression is via microRNA modulation. Indeed, recent studies showed that fatty acids are important regulators of microRNAs in the liver [29]. However, such analysis remains to be carried out in HCC cells. Rictor expression is known to be regulated by some miRNAs, such as miR-218 [30] and miR-155 [31]. Thus, it would be important to further test whether FASN regulates the expression of these microRNAs, thus modulating Rictor expression in HCC.

The present findings might have pivotal clinical implications. Indeed, the dependence of *AKT*-overexpressing cells on *de novo* lipogenesis might render these cells "metabolically vulnerable" to inhibitors of fatty acid biosynthesis. Of note, a number of FASN inhibitors have been developed to treat obesity and are generally well tolerated by the patients [12,30]. Some of these inhibitors showed encouraging anti-neoplastic effects in many experimental tumor models [3,4,30]. Thus, it might be envisaged that FASN inhibitors are effective in the treatment of at least a subgroup of human HCC characterized by the activation of the AKT pathway. As Rictor is directly regulated by FASN, overexpression of Rictor might represent a valuable marker for HCC that could benefit from anti-FASN therapeutic approaches.

Supplementary Material

Refer to Web version on PubMed Central for supplementary material.

Acknowledgments

Financial support: This work was supported by grant from the Italian Association Against Cancer (AIRC; grant number IG 12139) to DFC; NIH R01CA136606 and R03CA165122 to XC; grant P30DK026743 for UCSF Liver Center; grant from the Deutsche Forschungsgemeinschaft DFG (grant number Ev168/2-1) to ME.

List of Abbreviations

ACAC	acetyl-CoA carboxylase
ACLY	adenosine triphosphate citrate lyase
AKT	v-akt murine thymoma viral oncogene homolog
ELOVL5	elongation of very long chain fatty acids protein 5
FASN	fatty acid synthase
HCC	hepatocellular carcinoma
LDH	lactate dehydrogenase
mTOR	mammalian target of rapamycin
mTORC	mTOR complex
N-Ras	neuroblastoma Ras viral oncogene homolog
PKM2	pyruvate kinase M2 isoform
Raptor	regulatory-associated protein of mTOR

Rictor	rapamycin-insensitive companion of mTOR
Rps6	ribosomal protein S6
Scd1	stearoyl-CoA desaturase 1
siRNA	small interfering RNA

References

1. Menendez JA, Lupu R. Fatty acid synthase and the lipogenic phenotype in cancer pathogenesis. Nat Rev Cancer. 2007; 7:763–777. [PubMed: 17882277]
2. Zaidi N, Lupien L, Kuemmerle NB, Kinlaw WB, Swinnen JV, Smans K. Lipogenesis and lipolysis: the pathways exploited by the cancer cells to acquire fatty acids. Prog Lipid Res. 2013; 52:585–589. [PubMed: 24001676]
3. Kuhajda FP. Fatty acid synthase and cancer: new application of an old pathway. Cancer Res. 2006; 66:5977–5980. [PubMed: 16778164]
4. Migita T, Ruiz S, Fornari A, Fiorentino M, Priolo C, Zadra G, et al. Fatty acid synthase: a metabolic enzyme and candidate oncogene in prostate cancer. J Natl Cancer Inst. 2009; 101:519–532. [PubMed: 19318631]
5. Vazquez-Martin A, Colomer R, Brunet J, Lupu R, Menendez JA. Overexpression of fatty acid synthase gene activates HER1/HER2 tyrosine kinase receptors in human breast epithelial cells. Cell Prolif. 2008; 41:59–85. [PubMed: 18211286]
6. Evert M, Schneider-Stock R, Dombrowski F. Overexpression of fatty acid synthase in chemically and hormonally induced hepatocarcinogenesis of the rat. Lab Invest. 2005; 85:99–108. [PubMed: 15543204]
7. Ribback S, Calvisi DF, Cigliano A, Sailer V, Peters M, Rausch J, et al. Molecular and metabolic changes in human liver clear cell foci resemble the alterations occurring in rat hepatocarcinogenesis. J Hepatol. 2013; 58:1147–1156. [PubMed: 23348238]
8. Yamashita T, Honda M, Takatori H, Nishino R, Minato H, Takamura H, et al. Activation of lipogenic pathway correlates with cell proliferation and poor prognosis in hepatocellular carcinoma. J Hepatol. 2009; 50:100–110. [PubMed: 19008011]
9. Budhu A, Roessler S, Zhao X, Yu Z, Forgues M, Ji J, Karoly E, Qin LX, Ye QH, Jia HL, Fan J, Sun HC, Tang ZY, Wang XW. Integrated metabolite and gene expression profiles identify lipid biomarkers associated with progression of hepatocellular carcinoma and patient outcomes. Gastroenterology. 2013; 144:1066–1075. [PubMed: 23376425]
10. Calvisi DF, Wang C, Ho C, Ladu S, Lee SA, Mattu S, et al. Increased lipogenesis, induced by AKT-mTORC1-RPS6 signaling, promotes development of human hepatocellular carcinoma. Gastroenterology. 2011; 140:1071–1083. [PubMed: 21147110]
11. Li C, Yang W, Zhang J, Zheng X, Yao Y, Tu K, et al. SREBP-1 has a prognostic role and contributes to invasion and metastasis in human hepatocellular carcinoma. Int J Mol Sci. 2014; 15:7124–7138. [PubMed: 24776759]
12. Wu YS, Bao DK, Dai JY, Chen C, Zhang HX, Yang Y, et al. Polymorphisms in genes of the de novo lipogenesis pathway and overall survival of hepatocellular carcinoma patients undergoing transarterial chemoembolization. Asian Pac J Cancer Prev. 2015; 16:1051–1056. [PubMed: 25735330]
13. Hao Q, Li T, Zhang X, Gao P, Qiao P, Li S, et al. Expression and roles of fatty acid synthase in hepatocellular carcinoma. Oncol Rep. 2014; 32:2471–2476. [PubMed: 25231933]
14. Gao Y, Lin LP, Zhu CH, Chen Y, Hou YT, Ding J. Growth arrest induced by C75, A fatty acid synthase inhibitor, was partially modulated by p38 MAPK but not by p53 in human hepatocellular carcinoma. Cancer Biol Ther. 2006; 5:978–985. [PubMed: 16855382]

15. Ho C, Wang C, Mattu S, Destefanis G, Ladu S, Delogu S, et al. AKT and N-Ras coactivation in the mouse liver promotes rapid carcinogenesis by way of mTOR, FOXM1/SKP2, and c-Myc pathways. Hepatology. 2012; 55:833–845. [PubMed: 21993994]
16. Carlson CM, Frandsen JL, Kirchhof N, McIvor RS, Largaespada DA. Somatic integration of an oncogene-harboring Sleeping Beauty transposon models liver tumor development in the mouse. Proc Natl Acad Sci U S A. 2005; 102:17059–17064. [PubMed: 16286660]
17. Tward AD, Jones KD, Yant S, Cheung ST, Fan ST, Chen X, et al. Distinct pathways of genomic progression to benign and malignant tumors of the liver. Proc Natl Acad Sci U S A. 2007; 104:14771–14776. [PubMed: 17785413]
18. Wang C, Cigliano A, Jiang L, Li X, Fan B, Pilo MG, et al. 4EBP1/eIF4E and p70S6K/RPS6 axes play critical and distinct roles in hepatocarcinogenesis driven by AKT and N-Ras proto-oncogenes in mice. Hepatology. 2015; 61:200–213. [PubMed: 25145583]
19. Chakravarthy MV, Pan Z, Zhu Y, Tordjman K, Schneider JG, Coleman T, Turk J, et al. "New" hepatic fat activates PPARalpha to maintain glucose, lipid, and cholesterol homeostasis. Cell Metab. 2005; 1:309–322. [PubMed: 16054078]
20. Postic C, Shiota M, Niswender KD, Jetton TL, Chen Y, Moates JM, et al. Dual roles for glucokinase in glucose homeostasis as determined by liver and pancreatic beta cell-specific gene knock-outs using Cre recombinase. J Biol Chem. 1999; 274:305–315. [PubMed: 9867845]
21. Chen X, Calvisi DF. Hydrodynamic transfection for generation of novel mouse models for liver cancer research. Am J Pathol. 2014; 184:912–923. [PubMed: 24480331]
22. Magee JA, Ikenoue T, Nakada D, Lee JY, Guan KL, Morrison SJ. Temporal changes in PTEN and mTORC2 regulation of hematopoietic stem cell self-renewal and leukemia suppression. Cell Stem Cell. 2012; 11:415–428. [PubMed: 22958933]
23. Laplante M, Sabatini DM. mTOR signaling in growth control and disease. Cell. 2012; 149:274–293. [PubMed: 22500797]
24. Tripathy S, Jump DB. ELOVL5 regulates the mTORC2-Akt-FOXO1 pathway by controlling hepatic cis-vaccenic acid synthesis in diet-induced obese mice. J Lipid Res. 2013; 54:71–84. [PubMed: 23099444]
25. Kamphorst JJ, Cross JR, Fan J, de Stanchina E, Mathew R, White EP, et al. Hypoxic and Ras-transformed cells support growth by scavenging unsaturated fatty acids from lysophospholipids. Proc Natl Acad Sci U S A. 2013; 110:8882–8887. [PubMed: 23671091]
26. Liu ZL, Mao JH, Peng AF, Yin QS, Zhou Y, Long XH, et al. Inhibition of fatty acid synthase suppresses osteosarcoma cell invasion and migration via downregulation of the PI3K/Akt signaling pathway in vitro. Mol Med Rep. 2013; 7:608–612. [PubMed: 23229760]
27. Li N, Bu X, Tian X, Wu P, Yang L, Huang P. Fatty acid synthase regulates proliferation and migration of colorectal cancer cells via HER2-PI3K/Akt signaling pathway. Nutr Cancer. 2012; 64:864–870. [PubMed: 22860766]
28. Wang HQ, Altomare DA, Skele KL, Poulikakos PI, Kuhajda FP, Di Cristofano A, et al. Positive feedback regulation between AKT activation and fatty acid synthase expression in ovarian carcinoma cells. Oncogene. 2005; 24:3574–3582. [PubMed: 15806173]
29. Hernando Boigues JF, Mach N. The effect of polyunsaturated fatty acids on obesity through epigenetic modifications. Endocrinol Nutr. 2015; 62:338–349. [PubMed: 26003266]
30. Li J, Li X, Wang J, Wang Y, Qiu H. MicroRNA-218 increases cellular sensitivity to Rapamycin via targeting Rictor in cervical cancer. APMIS. 2015; 123:562–570. [PubMed: 25908215]
31. Martin EC, Rhodes LV, Elliott S, Krebs AE, Nephew KP, Flemington EK, et al. microRNA regulation of mammalian target of rapamycin expression and activity controls estrogen receptor function and RAD001 sensitivity. Mol Cancer. 2014; 13:229. [PubMed: 25283550]
32. Kridel SJ, Lowther WT, Pemble CW 4th. Fatty acid synthase inhibitors: new directions for oncology. Expert Opin Investig Drugs. 2007; 16:1817–1829.

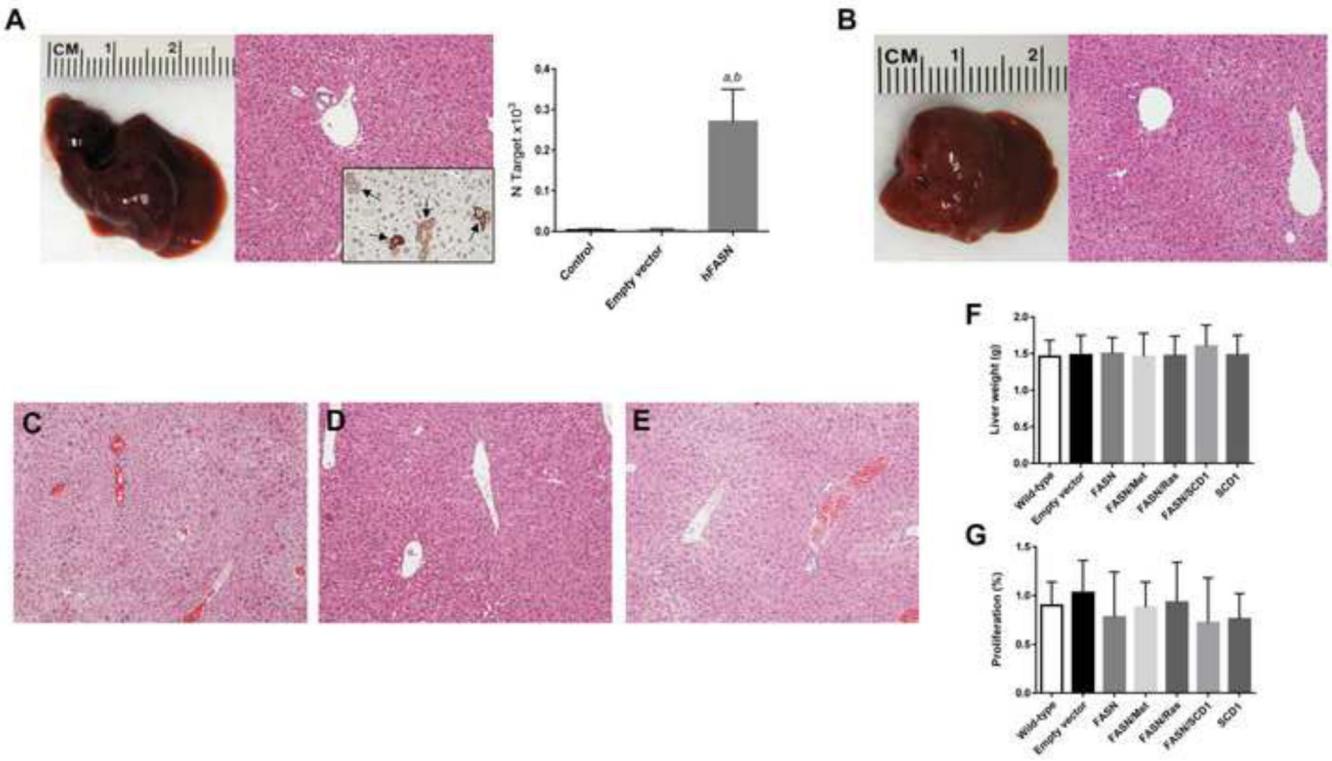

Fig. 1. *FASN* is not oncogenic in the mouse liver

(A) Macroscopic (*left panel*) and microscopic (*middle panel*) appearance of *FASN*-injected livers showing the absence of gross or histological alterations 40 weeks post hydrodynamic injection. Scattered cells positive for human (h)FASN were detected in FASN-injected livers (indicated by arrows; *inset*). Efficient transfection of *hFASN* was also detected by real-time RT-PCR in mouse livers (*right panel*). N target (NT) = $2^{-\Delta Ct}$, wherein ΔCt value of each sample was calculated by subtracting the average Ct value of the target gene from the average Ct value of the β-*actin* gene. Five samples per each mouse group were analyzed. Tukey-Kramer's test: P at least <0.001; *a*, versus control livers; *b*, versus livers injected with empty vector.

Analogously, concomitant overexpression of *FASN* with *c-Met* (B), *N-RasV12* (C) or *SCD1* (D), or overexpression of *SCD1* (E) alone was not oncogenic in the mouse liver. (F,G) Overexpression of FASN either alone or in association with the aforementioned genes did not induce changes in liver weight (F) or hepatocyte proliferation (G) when compared with wild-type (un-injected) or empty vector injected mice. Original magnification: 100× in A–E.

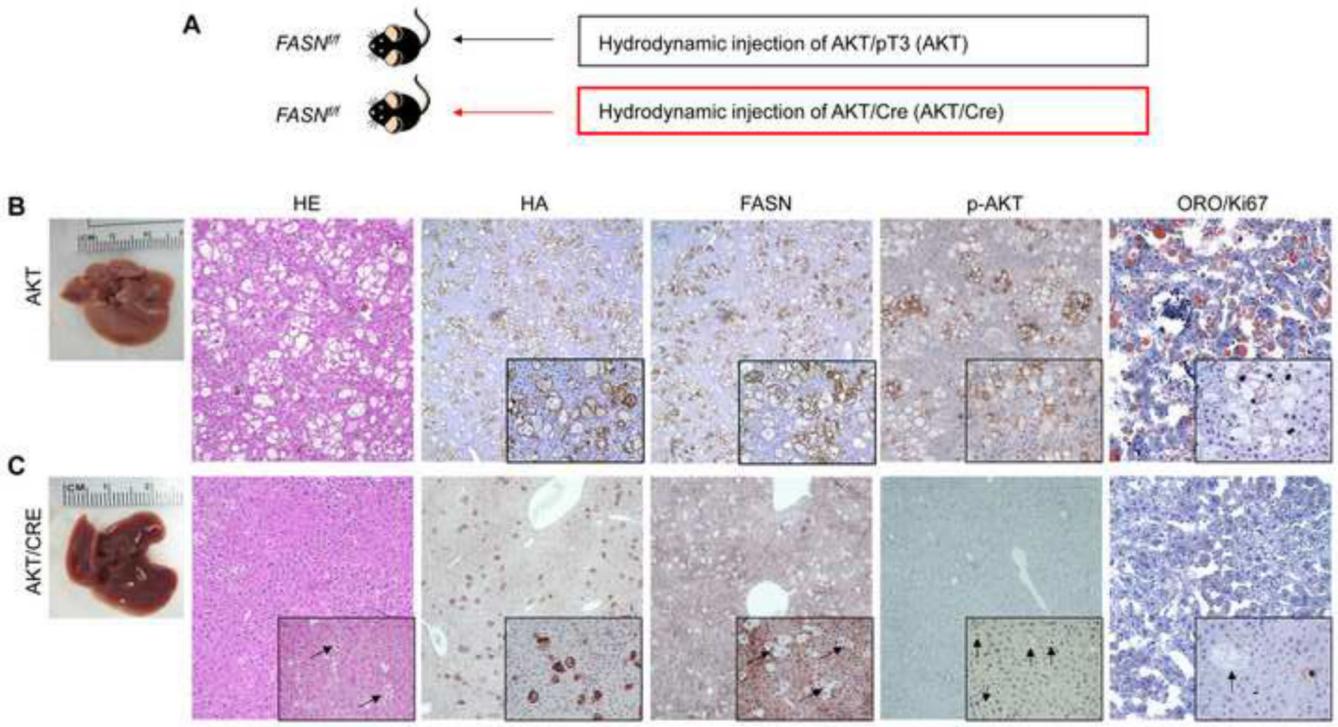

Fig. 2. Genetic ablation of FASN impairs lipid accumulation in mouse hepatocytes *in vivo*

(A) Scheme of the hydrodynamic gene delivery strategy. (B) Overexpression of *myr-AKT1* led to extensive lipid accumulation in *FASN*$^{fl/fl}$ mice retaining an intact *FASN* gene (indicated as AKT), 4 weeks post hydrodynamic injection. Macroscopically, livers from AKT mice were paler than wild-type livers, but did not show any appreciable parenchymal alteration. Microscopically, a strong immunoreactivity for the injected construct (HA-tag), FASN, and phosphorylated/activated (p-)AKT was detected. The elevated intracellular lipid storage was also underscored by the intense positivity for Oil-red-O (ORO) staining. In addition, the altered, lipid-rich hepatocytes showed an elevated proliferation rate, as assessed by Ki67 immunolabeling. (C) In striking contrast, Cre-mediated depletion of *FASN* gene in *FASN*$^{fl/fl}$ mice injected with *myr-AKT1* (indicated as AKT/Cre) abolished lipid accumulation in mouse hepatocytes at the same time point. Livers from AKT/Cre mice were equivalent to wild-type livers and showed only single, scattered cells with lipid accumulation (indicated by arrows and better appreciable in *insets*) that stained positive for HA-tag. Of note, the vast majority of lipid-rich hepatocytes transfected with HA-tag in AKT/Cre livers did not show immunolabeling for FASN, thus confirming the deletion of FASN by Cre recombinase. Immunolabeling for FASN was instead retained by the non-transfected, surrounding hepatocytes. Altered hepatocytes transfected with HA-tag in AKT/Cre mice also exhibited very weak or no staining for p-AKT, and only few of them were positive for Ki67 (the arrow indicates an enlarged, transfected hepatocyte showing absence of Ki67 staining, while another transfected cells displays positive immunoreactivity for the same protein). Furthermore, ORO staining did not provide an appreciable signal in AKT/Cre mice. Original magnifications: 100× in HE, HA, and FASN; 200× in insets and ORO staining.

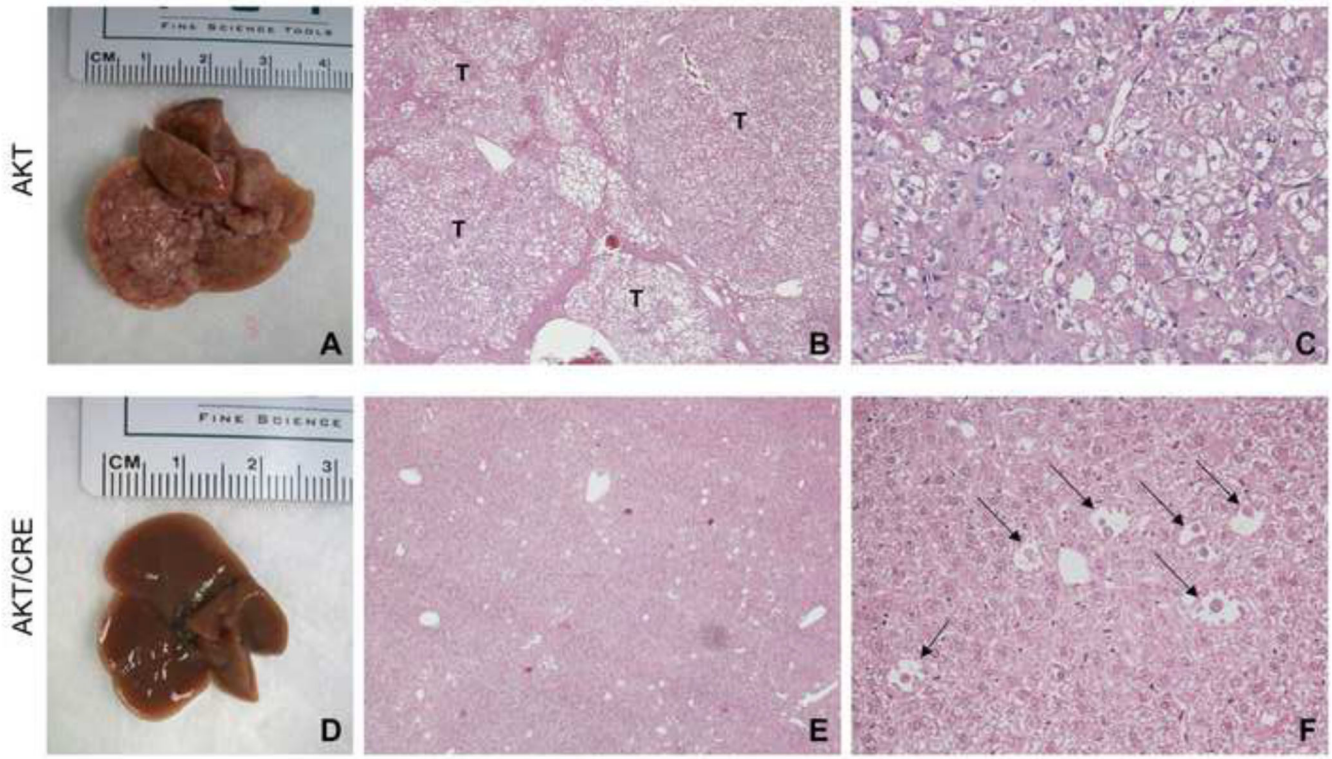

Fig. 3. Genetic ablation of FASN abolishes AKT-driven hepatocarcinogenesis in mice

(A–C) Overexpression of *myr-AKT1* promoted the development of multiple liver tumors within 31 weeks post hydrodynamic injection in $FASN^{fl/fl}$ mice with an intact FASN gene (indicated as AKT). (A) Macroscopically, liver of AKT/FASN mice appeared pale, enlarged, and characterized by the presence of numerous nodules occupying most of its surface. (B) Microscopically, the liver parenchyma of AKT/FASN mice was occupied by numerous colliding hepatocellular tumors (T). (C) Hepatocellular tumors were mainly composed of malignant cells with an enlarged, clear cytoplasm owing to lipid accumulation. (D–F) In striking contrast, Cre-mediated depletion of *FASN* gene in $FASN^{fl/fl}$ mice injected with *myr-AKT1* (indicated as AKT/Cre) completely inhibited carcinogenesis. Livers of AKT/Cre mice did not show any alteration macroscopically (D), whereas microscopically few, lipid rich hepatocytes were observed (E,F). Original magnifications: 40× in B and E; 200× in C and F. Abbreviation: HE, hematoxylin and eosin staining.

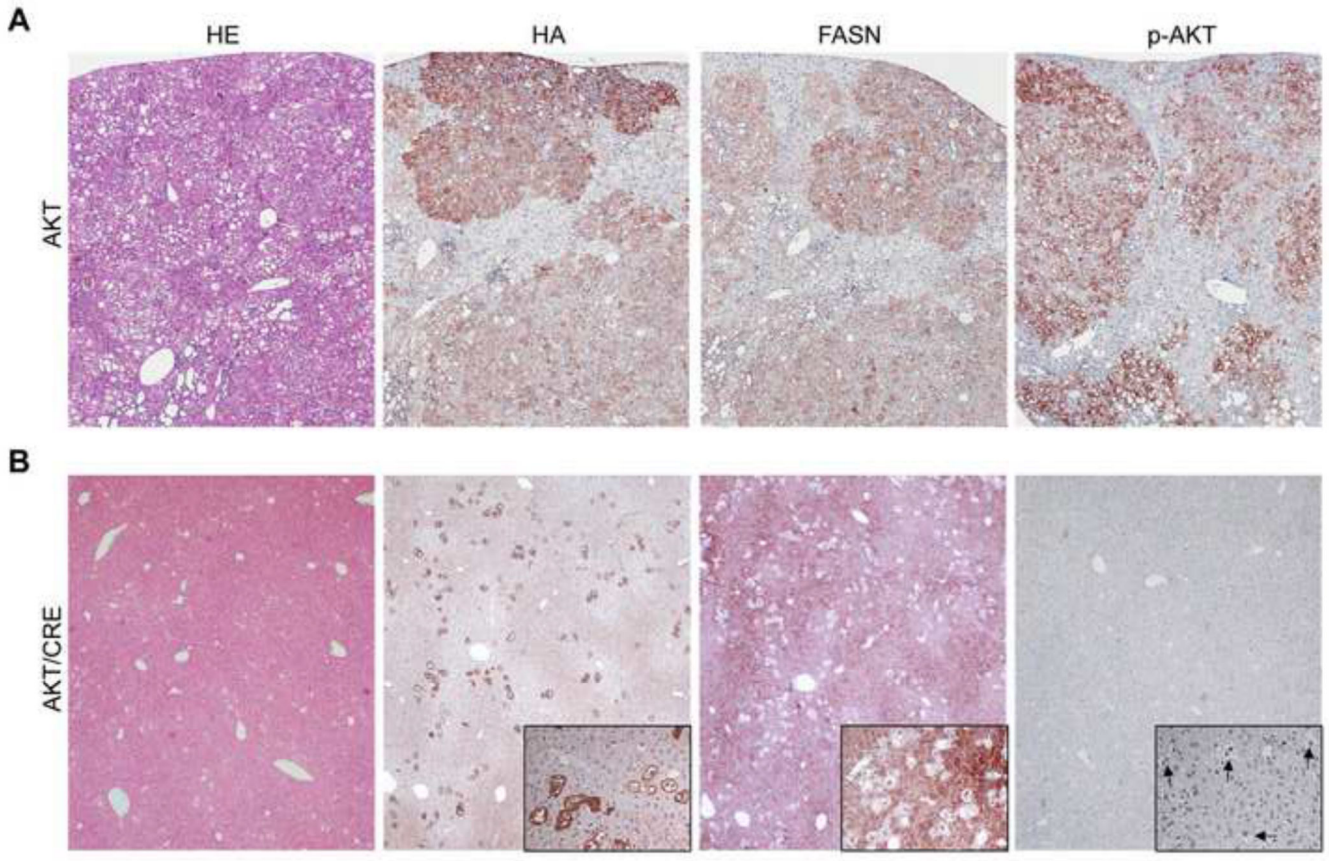

Fig. 4. Suppression of hepatocarcinogenesis following FASN deletion is accompanied downregulation of phosphorylated/activated AKT in the mouse liver

(A) Overexpression of *myr-AKT1* resulted in the development of multiple liver tumors by 31 weeks post hydrodynamic injection in *FASN*$^{fl/fl}$ mice with an intact FASN gene (indicated as AKT). These tumors and preneoplastic lesions were homogeneously immunoreactive for HA-tagged myr-AKT1 (HA), implying their origin from the transfected cells. In addition, preneoplastic and neoplastic lesions exhibited strong immunolabeling for phosphorylated/activated AKT (p-AKT) and FASN. (B) Noticeably, Cre-mediated depletion of the *FASN* gene in *FASN*$^{fl/fl}$ mice injected with *myr-AKT1* (indicated as AKT/Cre) completely abolished tumor development. Indeed, only few, altered cells positive for HA-tagged myr-AKT1 were detected in the livers of AKT/Cre mice. Importantly, most lipid-rich hepatocytes transfected with HA-tag in AKT/Cre livers did not show immunolabeling for FASN, thus confirming the deletion of FASN by the Cre recombinase. Immunolabeling for FASN was instead retained by the non-transfected hepatocytes. Altered hepatocytes transfected with HA-tag in AKT/Cre mice also exhibited very weak or no staining for p-AKT (altered cells are indicated by arrows in *insets*). Original magnification: 40×.

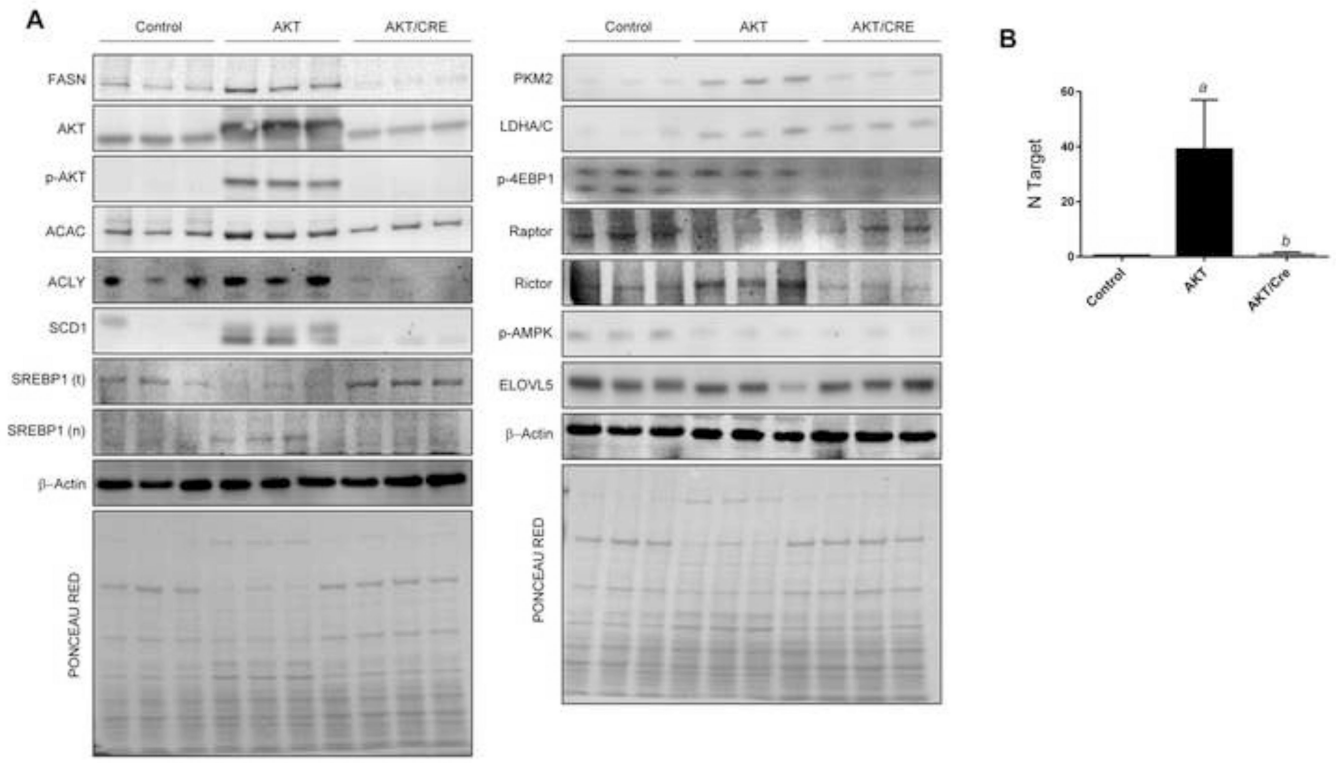

Fig. 5. Suppression of hepatocarcinogenesis following *FASN* deletion is accompanied downregulation of activated AKT and Rictor in the mouse liver

(A) Representative Western blot analysis of livers from control (*FASN*$^{fl/fl}$ mice injected with empty vector) mice, *FASN*$^{fl/fl}$ mice injected with *myr-AKT1* (AKT) and livers from *FASN*$^{fl/fl}$ mice injected with *myr-AKT1* and Cre (AKT/Cre) is shown. Deletion of FASN in AKT/FASN/Cre mice resulted in downregulation of phosphorylated/activated AKT at serine 472 (p-AKT) and Rictor. Levels of some AKT downstream effectors (ACLY, ACAC, SCD1, nuclear (n)SREBP1, LDHA/C, PKM2) were downregulated in AKT/Cre mice when compared with AKT mice. Four to six livers from each group of mice were used for the analysis, and representative images are shown. β-Actin and Ponceau Red reversible staining were used as loading controls (examples are shown in the bottom of the two blot panels). (B) Real-time RT-PCR analysis showing strong upregulation of *AKT1* in AKT livers when compared with control and AKT/Cre livers. N target (NT) = $2^{-\Delta Ct}$, wherein ΔCt value of each sample was calculated by subtracting the average Ct value of the target gene from the average Ct value of the β-*actin* gene. Four to six mice per each group were analyzed. Tukey-Kramer's test: P at least <0.001; *a*, versus control livers; *b*, versus AKT livers.

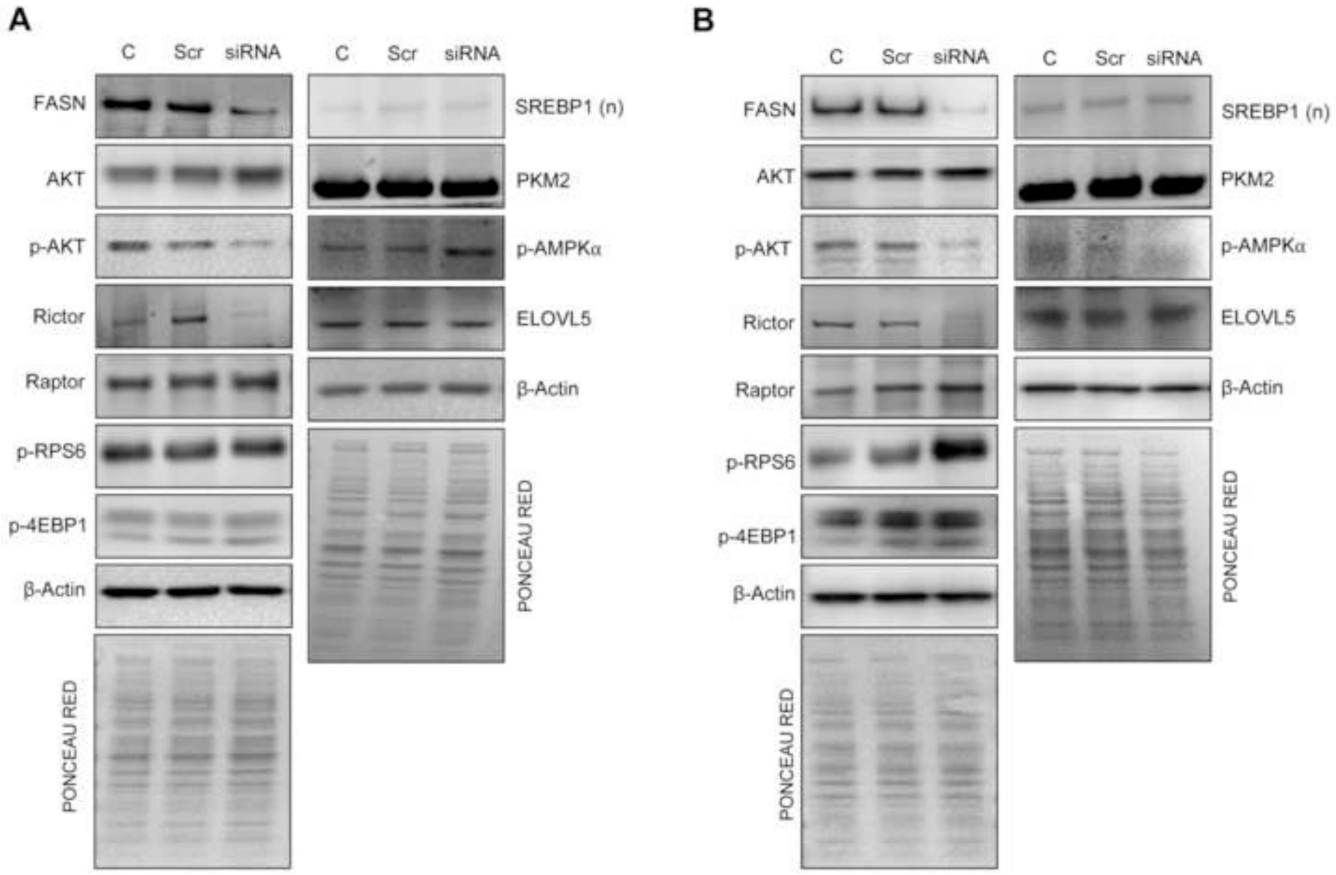

Fig. 6. Molecular consequences of FASN suppression in human hepatoma cell lines

(A) In HLF cells, FASN silencing via specific siRNA resulted in the downregulation of phosphorylated/activated AKT at serine 473 and Rictor, as detected by Western blot analysis (A; *left panel*). Equivalent results were obtained in HepG2 cells (B; *left panel*). For Western blot analysis, β-Actin and Ponceau Red reversible staining were used as loading controls (examples are shown in the bottom of the blot panels).

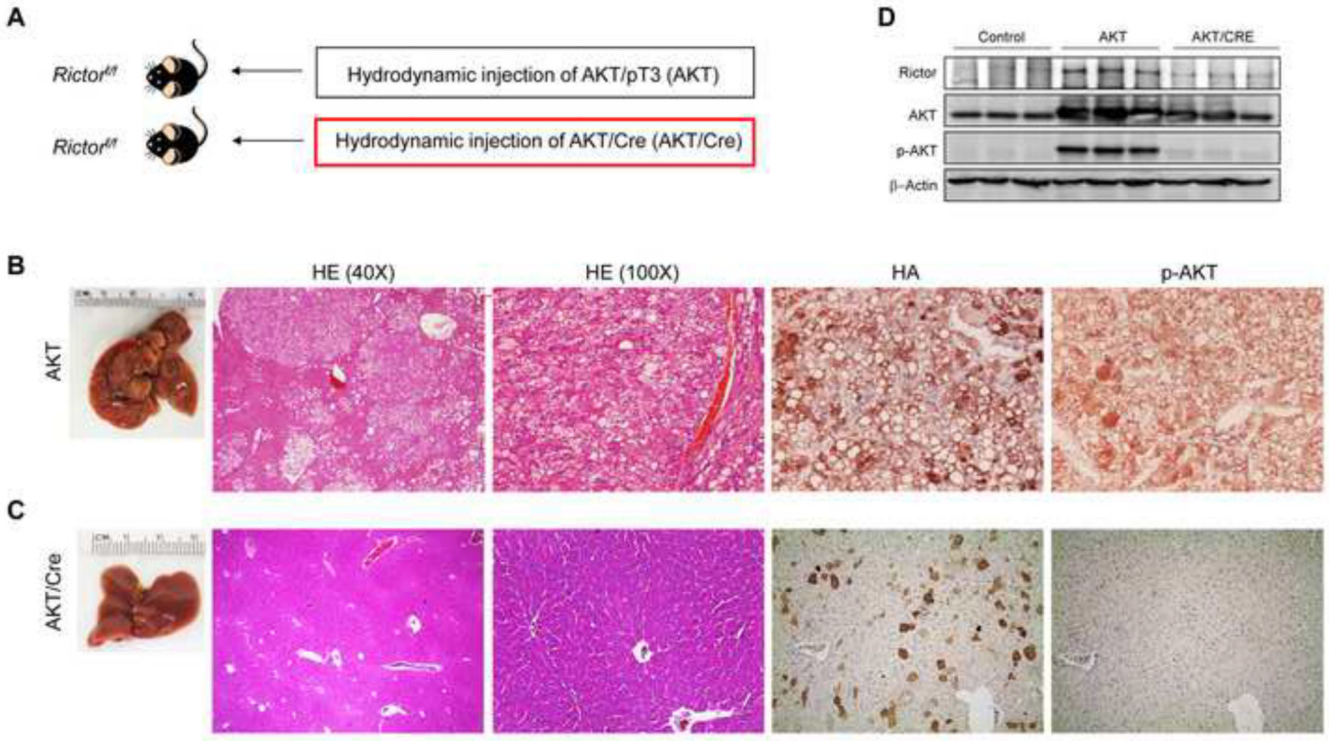

Fig. 7. Genetic ablation of Rictor abolishes AKT-driven hepatocarcinogenesis in mice

(A) Scheme of the hydrodynamic gene delivery strategy. (B) Overexpression of *myr-AKT1* promoted the development of multiple liver tumors by 22 weeks post hydrodynamic injection in *Rictor*$^{fl/fl}$ mice with an intact *Rictor* gene (indicated as AKT). Macroscopically, livers of AKT mice were enlarged with several nodules emerging in the parenchyma. Microscopically, livers of AKT mice were occupied by numerous hepatocellular tumors, which were mainly composed of malignant cells with an enlarged, clear cytoplasm owing to lipid accumulation, and displaying strong immunolabeling for HA-tag and p-AKT. (C) In contrast, Cre-mediated depletion of *Rictor* gene in *Rictor*$^{fl/fl}$ mice injected with *myr-AKT1* (indicated as AKT/Cre) completely inhibited carcinogenesis. Livers of AKT/Cre mice did not show any alteration macroscopically, whereas microscopically few, lipid rich hepatocytes were observed. These hepatocytes were positive for HA-tag but not for p-AKT. Original magnifications: 40× in HE; 100× in HE, HA, and p-AKT. Abbreviation: HE, hematoxylin and eosin staining. (D) Western blotting showing the abolishment of AKT activity in AKT/Cre mouse livers.

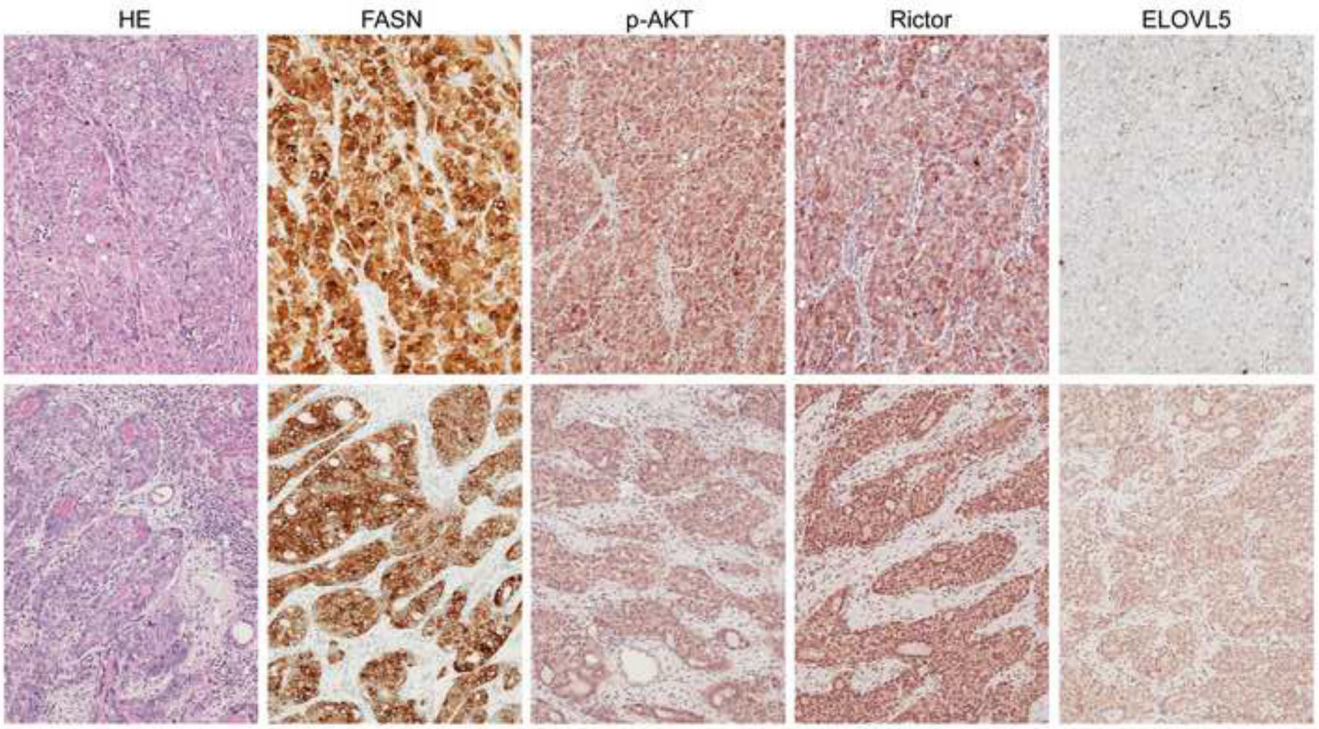

Fig. 8. Immunohistochemical patterns of FASN, activated/phosphorylated AKT, Rictor, and ELOVL5 in human hepatocellular carcinoma (HCC)

Upper panel: HCC specimen showing strong immunolabeling for FASN, activated/phosphorylated AKT (p-AKT), and Rictor, whereas does not exhibit immunoreactivity for ELOVL5. Lower panel: HCC specimen with strong immunoreactivity for FASN, p-AKT, Rictor, and ELOVL5. Abbreviation: HE, hematoxylin and eosin staining. Original magnification: 200× in all pictures.